Engineering Design of Breakwater Structures for Coastal Erosion Mitigation: A Case Study in Sragi, South Lampung

Suciana[1*], Mustarakh Gelfi[1], and Pandu Nababan[1]
[1]Ocean Engineering Department, Institut Teknologi Sumatera, Lampung, Indonesia
*E-mail address: suciana@kl.itera.ac.id

ABSTRACT

Kuala Jaya Beach, located in Bandar Agung Village, Sragi District, South Lampung, is experiencing severe coastal erosion, leading to shoreline retreat and degradation of coastal ecosystems. This study presents the engineering design of breakwater structures as a mitigation strategy. The design process considered key parameters, including significant wave height and period, Highest High Water Level (HHWL), wave refraction and breaking coefficients, wave set-up, projected sea level rise, wave run-up, and structural stability based on Terzaghi and Hudson equations. Wave characteristics were analyzed using a Weibull distribution for a 50-year return period, yielding a significant wave height of 2.26 m and a period of 6.98 s. Tidal analysis used the Admiralty method to determine an HHWL of 0.63 m. Three types of armor layers were evaluated: natural rock, concrete cubes, and geobags. The resulting crest widths were 2.0 m, 1.8 m, and 2.8 m, with corresponding elevations of 3.76 m, 3.0 m, and 3.6 m. Two breakwaters, 1000 m and 800 m in length, were positioned at a depth of 5 m near the wave-breaking zone. Stability analysis showed armor to secondary layer ratios of 2.4 for concrete cubes and 2.0 for natural rock. All designs allow controlled seepage, dissipating wave energy, and effectively preventing further shoreline retreat. Among the three armor types evaluated, natural rock is recommended as the most suitable option for Sragi, as it provides reliable hydraulic stability and best fits the local site conditions.

Keywords: Breakwater, Coastal, Erosion, South Lampung

1. INTRODUCTION

Coastal zones are vital ecosystems that provide significant benefits to local communities, ranging from fisheries and salt farming to tourism, while supporting daily socio-economic activities. However, Indonesia's southern Lampung coast, Sragi District, faces escalating coastal erosion driven by wave action, currents, and wind. DSAS analysis indicates that Sragi's shoreline is actively changing, with erosion projected to reach –45.80 m and 134.319 ha of land loss by 2033, highlighting the severe risk of coastal retreat in the next decade [1]. In particular, a study in 2018-2020 reported a maximum shoreline retreat of ~217.6 m in Sragi [2]. This erosion undermines shoreline stability, degrades coastal ecosystems, and disrupts livelihoods [3][4]. The urgency in Sragi is heightened by the fact that much of its coastline is lined with residential areas, making erosion not only an environmental concern but also a direct threat to housing, community safety, and local infrastructure.

Global research has demonstrated that breakwater structures can significantly alter hydrodynamics and sediment dynamics. Submerged breakwaters influence coastal morphology by modifying wave energy and sediment transport patterns [5], while detached breakwaters in Indonesia have shown distinct effects on sediment accumulation and shoreline configuration [6]. numerical modeling has quantified the influence of breakwaters on sediment redistribution

under various wave regimes [7] and experimental studies show that breakwater geometry affects bed morphology, balancing erosion at the toe with accretion behind the structure [8].

Despite these advances, a localized gap remains in optimizing breakwater design, particularly in determining dimensions, configurations, and material selection tailored to the hydrodynamic and socio-environmental context of Sragi's coastline. This study aims to address that gap by designing breakwater structures suited to Sragi's environmental and social conditions, incorporating wave parameters, tidal dynamics, and structural stability. The hypothesis is that a properly designed breakwater will effectively dissipate wave energy, reduce erosion, and protect both coastal ecosystems and the residential communities along the Sragi shoreline.

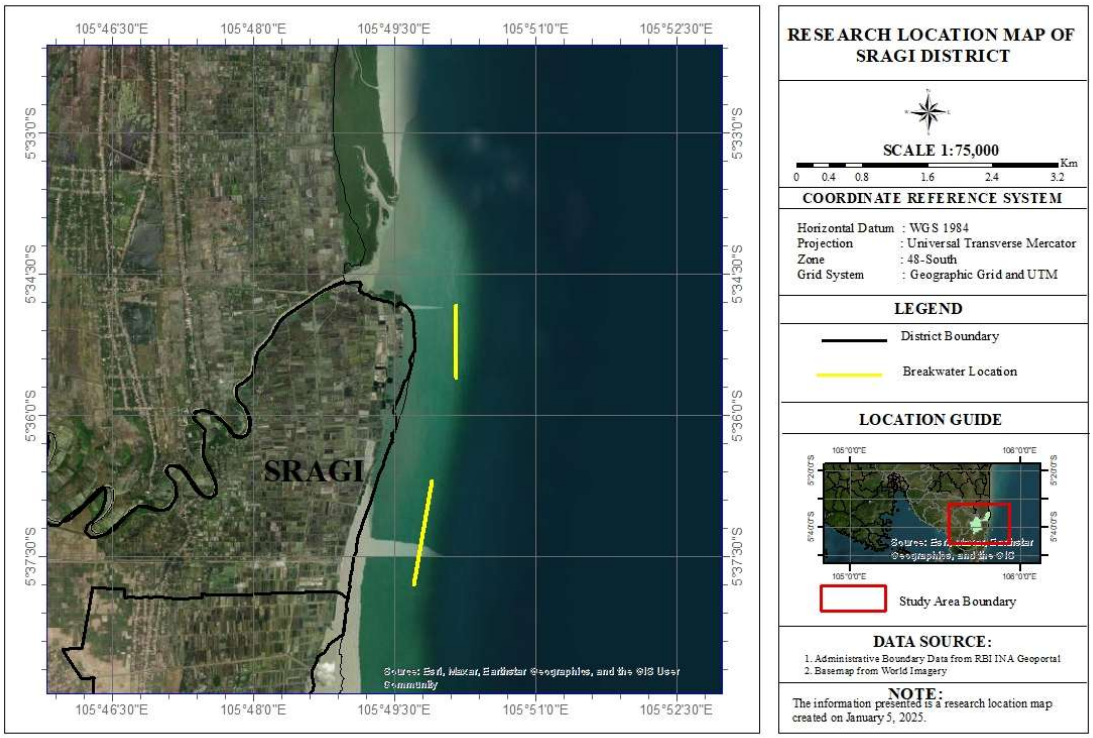

Figure 1. Location of Sragi, South Lampung

2. THEORY AND METHODS

2.1 Statistical Method

For a constant return period, both wave height and wave period generally exhibit an increasing trend over time. Incorporating a larger dataset into the analysis enhances the precision of the resulting predictions, as greater data availability improves both the statistical probability and the reliability of the analysis outcomes. In this study, Equation (1) is applied within the framework of the Weibull method:

$$P\,(H_s \le H_{sm}) = 1 - \frac{m - 0{,}2 - \frac{0.27}{\sqrt{k}}}{N_T + 0.2 + \frac{0.23}{\sqrt{k}}} \quad (1)$$

P (Hs ≤ Hsm) represents the probability that the representative wave height (Hs) does not exceed the wave height at the m-th rank (Hsm), where m denotes the order of the significant wave, NT indicates the total number of wave events during the observation period. The calculation in the linear regression analysis, based on the value of ym, can be determined using Equation 2

$$y_m=[-In\{1- P (H_s\leq H_{sm})\}]^{\frac{1}{k}} \quad (2)$$

The value of yr for the significant wave height can be determined using Equation 3

$$y_r=\{-In (L T_r)\}^{1/k} \quad (3)$$

where ym is the reduction factor in the Weibull method. Wave height or wave period can be determined from the probability distribution function using Equations (4) through (7).

$$H_{sm} =Ay_m+B \quad (4)$$

$$A = \frac{n\sum H_{sm}y_m - \sum H_{sm}\sum y_m}{n\sum y_m^{\,2} - (\sum y_m)^2} \quad (5)$$

$$B = \bar{X}H_{sm} - A\times\bar{X}y_m \quad (6)$$

$$H_{sr} =Ay_r+B \quad (7)$$

where A and B are the estimated values of the scale and location parameters, obtained from the linear regression analysis. Confidence intervals can be applied in the analysis of extreme wave heights, which are influenced by the data distribution and the standard deviation value [9]. The formula for calculating the normalized standard deviation is given in Equations (8) to (10). The empirical coefficients for determining the return period are presented in Table 1.

$$\sigma H_s = \left[\frac{1}{N-1}\sum_{i=1}^{N}(H_{sm}-\bar{X}H_{sm})^2\right]^{\frac{1}{2}} \quad (8)$$

$$\sigma_{nr} = \frac{1}{\sqrt{N}}\left[1 + \alpha(y_r - c + \varepsilon \, In \, v\right]^{\frac{1}{2}} \quad (9)$$

$$\alpha = \alpha_1 e^{\,a_2 N^{-1,3+k\sqrt{-In\,v}}} \quad (10)$$

Table 1. Empirical Coefficient Values for Return Period [12]

Distribution	α_1	α_2	ε	c	K
FT-1	0.64	9.0	0.93	0	1.33
***Weibull* (k = 0,75)**	1.65	11.4	-0.63	0	1.15
***Weibull* (k = 1,0)**	1.92	11.4	0.00	0.3	0.90
***Weibull* (k = 1,4)**	2.05	11.4	0.69	0.4	0.72
***Weibull* (k = 2,0)**	2.24	11.4	1.34	0.5	0.54

The k value indicates the shape of the Weibull distribution curve [10]. The selection of the return period is adjusted according to the type of structure or construction to be designed, while

also considering whether the location is part of a conservation area [11]. For further analysis, the confidence interval limits provided in Table 2 are required.

Table 2. The confidence interval limits provided [12]

Confidence Level (%)	Confidence Interval Limit for H_{sr}	Upper Limit Exceedance Probability (%)
80	1.28 σ_r	10
85	1.44 σ_r	7.5
90	1.65 σ_r	5
95	1.96 σ_r	2.5
99	2.58 σ_r	0.5

2.2.Wave and Tide

Wave characteristics occur as waves travel from deep water into shallow water. Factors influencing these changes include refraction, shoaling, diffraction, and reflection. These processes affect both wave height and the pattern of wave crests at a given coastal location. The refraction coefficient and shoaling coefficient can be obtained using Equations (11) and (12). K_r is the refraction coefficient, α_0 is the angle formed between the deep-water wave crest and the shoreline and α is the angle formed between the wave crest and the seabed contour line at the observed point. In analyzing wave deformation, the deep-water wave height without refraction can be considered. The formula used to calculate the deformed wave height is given in Equation (13). where H'_0 is the deformed wave height or equivalent deep-water wave height, H_0 is the deep-water wave height, and K_s is the shoaling coefficient.

$$K_r=\sqrt{\frac{\cos\alpha_0}{\cos\alpha}} \tag{11}$$

$$K_s=\sqrt{\frac{n_0 \times L_0}{n_L}} \tag{12}$$

$$H'_0=K_s\times K_r\times H_0 \tag{13}$$

Waves generally occur as waves approach the shore, where the wave crest sharpens and the water depth reaches approximately one-quarter of the wave height, eventually causing the wave to break. Changes in seabed depth can increase wave height as waves enter shallow water. Based on the table of d/L values, different breaking wave heights can be determined. This calculation refers to the graph that illustrates the relationship between H'_0/gT^2 dan H_b/gT^2 [13], The breaking wave height H_b is obtained from the plot between H'_0/gT^2 and the beach slope (m). Based on the table of d_b/H_b dan H_b/gT^2, the relationship can be used to determine various seabed slopes.

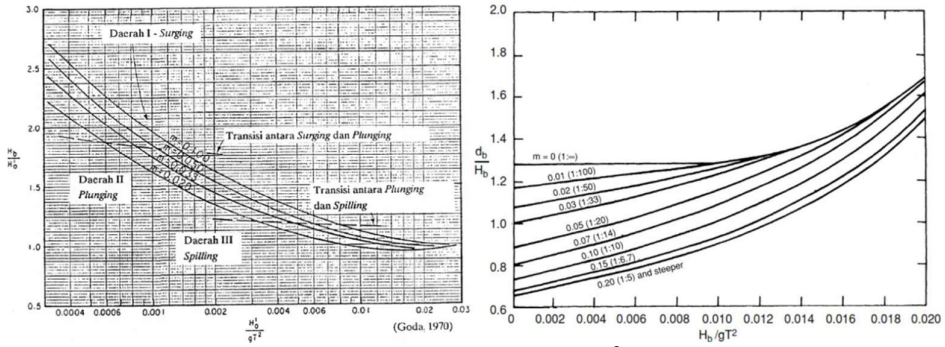

Figure 2. Relationship between Hb/H'$_0$ and H'$_0$/gT^2(Left) Relationship between d_b/H_b and H_b/gT^2 (Right) [14]

Tides are the periodic fluctuations in sea level caused by the gravitational pull between the Earth, Moon, and Sun on the ocean's water mass. These changes occur in a specific cycle, generally referred to as a tidal cycle. Several factors, such as geographical location, coastal morphology, and water bathymetry, influence the tidal characteristics of a region [15]. To determine the tidal type of a region, the formzahl number is used, which is the ratio between the amplitude of the principal diurnal tidal constituents and the amplitude of the principal semidiurnal tidal constituents. The equation for the formzahl number is given in Equation (14).

$$F=\frac{O_1+K_1}{M_2+S_2} \tag{14}$$

The Admiralty Method is an approach used to analyze tidal data, with the advantage of being able to process short-term data, whether over 15 days or 29 days. This method can calculate the tidal constants needed to determine the tidal type and the mean sea level elevation [16].

2.3. Breakwater Design Method

The purpose of DWL (Design Water Level) planning is to ensure that the structure can withstand dynamic changes in water level influenced by various factors such as tides, rainfall, or weather changes [17]. The equation 15 used to determine DWL. SW is the sea level increase due to waves, SLR (Sea Level Rise) is the sea level height due to global temperature rise, and Δh is the sea level increase due to storm surge. Waves moving from the sea toward the shore cause changes in the water surface elevation in coastal areas, differing from the still water elevation [18]. Near the breaking wave point, the mean water level decreases compared to the still water elevation due to the effect of wave breaking, as calculated using Equation (16).

$$DWL = HHWL + S_w + SLR + \Delta h \tag{15}$$

$$S_w = 0{,}19\left[1\text{-}2{,}82\sqrt{\frac{H_b}{gT^2}}\right]H_b \tag{16}$$

In the planning process, the planned elevation is analyzed by considering the run-up height (R), which is the maximum wave height after the wave strikes the coastal protection structure [19] using Equation (17). where Ir is the Irribaren number, θ is the slope angle of the breakwater, H is the wave height at the coastal structure, and L0 is the deep-water wavelength. After obtaining the Irribaren number, it is plotted on a graph according to the planned structure type to determine the run-up (Ru) and run-down (Rd) values as shown in Figure 3. the maximum

elevation of the coastal protection structure is calculated using equation 18 . where DWL is the design water level elevation, Ru is the wave run-up, and Fb is the freeboard height (0.5 m).

$$I_r = \frac{\text{tg } \theta}{\left(\frac{H}{L_0}\right)^{0,5}} \tag{17}$$

$$\text{Elevation} = DWL + R_u + Fb \tag{18}$$

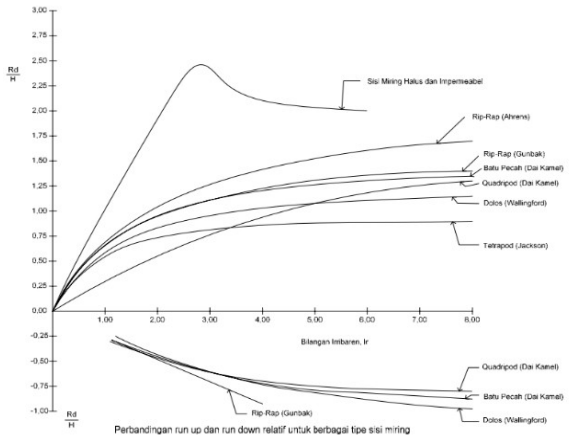

Figure 3. Graph of Wave Run-Up and Run-Down Values [14]

Coastal protection structures such as breakwaters are designed to reduce or dissipate waves before they reach the shoreline. In designing breakwater dimensions, several factors must be considered. The stability of the armor stone in coastal protection design is determined based on the weight of the armor unit. The equation 19 used is Hudson's formula, where W is the armor weight (newtons), H is the design wave height (m), γr is the unit weight of the armor (N/m³), and KD is the stability coefficient of the armor layer.

$$W = \frac{\gamma r \times H^3}{K_D \times (S_r\text{-}1)^3 \cot \theta} \tag{19}$$

The crest width of the coastal protection structure can be determined based on the allowable overtopping limit and operational requirements for equipment during maintenance and construction. Equation 20 is used to calculate the crest width, where B is the crest width (m), n is the number of layers, is the layer coefficient, W is the armor weight, and γr is the unit weight of the armor stone.

$$B = n\, K_\Delta \left(\frac{W}{\gamma r}\right)^{\frac{1}{3}} \tag{20}$$

Stone Diameter: In the breakwater layer, the required stone diameter is obtained using Equation (21). where is the stone diameter, W is the armor weight, and γr is the unit weight of the armor stone.

$$D_{n50}=\left(\frac{W}{\gamma r}\right)^{\frac{1}{3}} \quad (21)$$

Armor Layer Thickness: This serves to strengthen the crest of the structure, provide road access for maintenance, and increase the crest elevation. The thickness of the armor layer and the number of armor units per layer can be calculated using the equations 22. where t is the armor layer thickness, is the layer coefficient, W is the armor weight, n is the number of armor stone layers in the protection layer (minimum n = 2), A is taken as 10 m², and γr is the unit weight of the armor layer.

$$t = n\, K_{\Delta} \times \left(\frac{W}{\gamma_r}\right)^{\frac{1}{3}} \quad (22)$$

$$N = A\, n\, K_{\Delta} \times \left[1 \frac{P}{100}\right]\left(\frac{\gamma_r}{W}\right)^{\frac{2}{3}} \quad (23)$$

3. RESULTS AND DISCUSSION

The research Coastal engineering design requires a thorough understanding of local wave climate characteristics, as wave forces are a primary factor influencing the stability and longevity of shoreline protection structures. Long-term wave data analysis is therefore essential for determining design parameters that can withstand extreme conditions throughout the intended service life of a structure.The recapitulation of the 10-year significant wave height analysis is presented in Figure 4. In the return period analysis for the design wave, the Weibull distribution method was used to estimate the design wave height based on a specific return period. In this study, a design life of 50 years was considered, involving the ranking of the highest wave heights and periods. Tables 3 and 4 present the recapitulated results of the design wave analysis using the Weibull method.

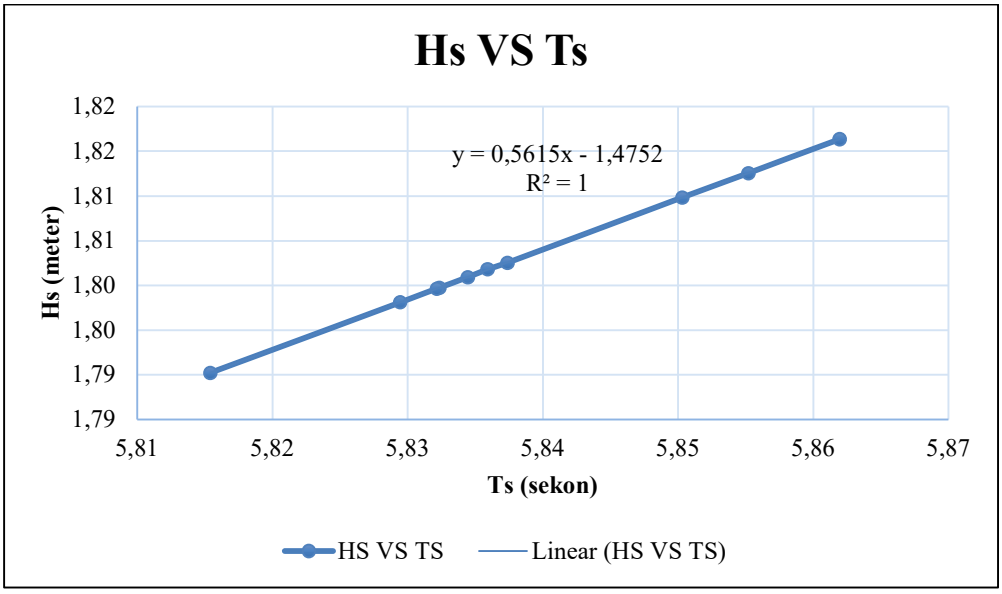

Figure 4. Graph of the relationship between Hs and Ts

From the data trends, it can be observed that the significant wave height (Hs) remains relatively consistent over the 10-year observation period, fluctuating only within a narrow range

of ±0.02 m. This stability suggests that the offshore wave climate in the study area has not experienced major interannual variations during the observation period. However, even small variations in Hs can have meaningful implications when projected over longer return periods, as reflected in the Weibull analysis results. The strong correlation between Hs and the significant wave period (Ts) in Figure 4 indicates that wave energy conditions are largely controlled by prevailing wind regimes and fetch length, which is consistent with the regional meteorological patterns. The Weibull-based projections provide a statistically robust basis for determining extreme design conditions, which is essential for ensuring the structural integrity and service life of coastal protection measures.

Table 3. Results of the Weibull method calculation for parameters A and B

m	Year	Hsm	P	ym	Hsm.ym	ym^2	h-h	$\hat{A}$	$\hat{B}$
1	2023	1.81	0.94	4.21	7.65	17.7	1.00	0.4	2.4
2	2018	1.81	0.85	2.74	4.98	7.54	1.00		
3	2019	1.81	0.75	2.03	3.68	4.13	1.00		
4	2021	1.80	0.65	1.55	2.80	2.42	1.00		
5	2014	1.80	0.56	1.20	2.16	1.44	0.99		
6	2017	1.80	0.46	0.91	1.64	0.83	0.99		
7	2016	1.80	0.37	0.67	1.21	0.45	0.99		
8	2020	1.80	0.27	0.46	0.84	0.22	0.99		
9	2022	1.79	0.18	0.28	0.52	0.08	0.99		
10	2015	1.79	0.08	0.12	0.23	0.01	0.99		
Total		18.0	5.15	14.2	19.1	34.9	10.0		
Average		1.80	0.51	1.42	2.57	3.49	1		

Table 4. Results of the design wave (Hsr) calculation for return period

Return Period (Tr)	yr	Hsr	σnr	σHs	σr	Hsr-1,28σr	Hsr+1,28σr
10	0.23	2.3	0.3	1.65	0.5	1.66	**3.01**
25	0.32	2.2	0.3		0.5	1.63	**2.96**
50	0.39	2.2	0.3		0.5	1.58	**2.94**

The refraction coefficient was calculated using Equation (11), yielding a value of 0.99. The shoaling coefficient (Ks), determined from the d/L_o ratio, was found to be 0.952. Using Equation (13), the equivalent deep-water wave height (H'_o) was calculated to be 2.32 m. Based on the analysis in Table 5, which spans depths from 1 meter to 25 meters, the refraction coefficient (Kr) was determined to be 1.00. From the d/L_o value of 0.070, the shoaling coefficient (Ks) was calculated as 0.97, resulting in a deformation wave height of 1.26 m. A Kr value close to unity indicates that wave direction remained essentially unchanged as the wave propagated toward the shore, meaning refraction effects were negligible in altering wave approach. Conversely, Ks values slightly below 1.0 signify minor attenuation of wave height due to shoaling, caused by the redistribution of wave energy as water depth decreases. The resulting deformation wave height reflects the net transformation after both refraction and shoaling processes. This transformed height is critical for accurately estimating breaking wave conditions, predicting nearshore energy levels, and ensuring the stability and reliability of coastal protection structures under design storm conditions.

Table 5. Recapitulation of Wave Refraction Analysis Results

D	a0	Hs	Ts	L0	d/L0	d/L	L	c0	c	sin a0	sin a	a	cos a0	cos a	Kr	Ks	H'0 (m)
25	24	2.4	6.99	76.1	0.33	0.34	74.06	10.90	10.6	0.41	0.40	23.6	0.91	0.92	1.00	0.96	2.33
20	53.1	2.3	6.99	74.0	0.27	0.29	70.08	10.60	10.0	0.80	0.76	49.2	0.60	0.65	0.96	0.94	2.10
15	23.0	2.10	6.99	70.0	0.21	0.24	63.30	10.03	9.06	0.39	0.35	20.6	0.92	0.94	0.99	0.92	1.92
10	12.0	1.92	6.99	63.3	0.16	0.19	52.64	9.06	7.53	0.21	0.17	9.96	0.98	0.98	1.00	0.91	1.75
5	6.1	1.75	6.99	52.6	0.09	0.14	36.60	7.53	5.24	0.11	0.07	4.24	0.99	1.00	1.00	0.94	1.64
4	5.9	1.64	6.99	36.6	0.11	0.15	26.89	5.24	3.85	0.10	0.08	4.36	0.99	1.00	1.00	0.93	1.51
3	8.1	1.51	6.99	26.8	0.11	0.15	19.94	3.85	2.85	0.14	0.10	6.01	0.99	0.99	1.00	0.93	1.40
2	4.20	1.40	6.99	19.9	0.10	0.14	14.19	2.85	2.03	0.07	0.05	2.99	1.00	1.00	1.00	0.93	1.30
1	7.60	1.30	6.99	14.1	0.07	0.11	8.78	2.03	1.26	0.13	0.08	4.69	0.99	1.00	1.00	0.97	1.26

Breaking waves occur when waves travel from deep to shallow water, which have reached their maximum point, causing wave breaking and changes in the wave crest shape. The following is the recapitulated calculation result for breaking wave depth at a depth of 5 meters, presented in Table 6. The coastal structure is planned to be built at an elevation of 5 meters with a beach slope of 0.003, resulting in a breaking wave height of 1.64 meters. The breaking depth obtained was 1.28 meters, with a travel distance of 852 meters during the breaking process, categorized as a spilling breaker.

Table 6. Recapitulation of Breaking Wave Depth

Pias	H (m)	T (s)	L0 (m)	Ic (m)	Δh (m)	m	Ho/gT^2	Hb/H'0	Hb (m)	Hb/gT^2	db/Hb	db (m)	Iribarren number	Type	Distance (m)
1	1.64	6.99	52.64	5	1738	0.003	0.0034	1.17	1.915	0.0040	1.28	2.45	0.02	Spilling	852
2	1.71	6.99	76.17	5	2480	0.002	0.0036	1.20	2.048	0.0043	1.28	2.62	0.01	Spilling	1300
1 (h1)	1.26	6.99	14.19	1	1173	0.001	0.0026	1.25	1.577	0.0033	1.28	2.02	0.003	Spilling	2367
2 (h1)	1.33	6.99	14.27	1	922	0.001	0.0028	1.275	1.695	0.0035	1.28	2.17	0.004	Spilling	2001

A tidal analysis was carried out with the objective of obtaining the sea surface elevation, specifically the Highest High Water Level (HHWL), which will later be used to determine the design water level for the coastal protection structure planning. Based on the calculation results, the formzahl value obtained was 0.72 which falls into the classification of mixed tides leaning towards semidiurnal tides ($0.25 < F \leq 1.50$).

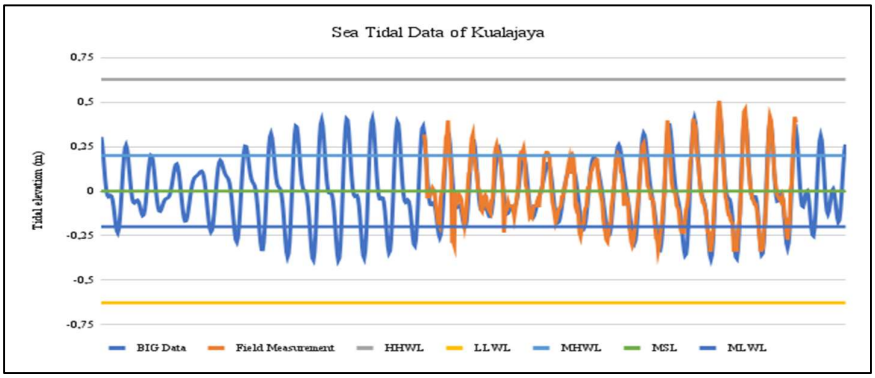

Figure 5. Tide data in Sragi South Lampung

In selecting the coastal protection structure, a decision table was created based on several chosen criteria with assigned weights and options for different types of coastal protection

structures. The scores used for selecting the coastal protection structure range from 0 to 5. The decision table for various selection criteria is presented in Table 7.

Table 7. Selection of Coastal Protection Structure

Criteria	Weight%	Option											
		Do nothing		Setback		Revetment		Breakwater		Groin		Jetty	
Location	20%	0	0	0	0	2	0.4	5	1	1	0.2	1	0.2
Longshore Erosion	20%	0	0	0	0	5	1	5	1	1	0.2	1	0.2
Soil Type	10%	3	0.3	3	0.3	3	0.3	4	0.4	2	0.2	2	0.2
Coastal used	20%	4	0.8	4	0.8	3	0.6	4	0.8	2	0.4	2	0.4
Quarry Materials	10%	3	0.3	3	0.3	4	0.4	4	0.4	3	0.3	3	0.3
Total Population	20%	0	0	0	0	3	0.6	5	1	2	0.4	2	0.4
			1.4		1.4		3.3		4.6		1.7		1.7

Based on the decision table, the breakwater was identified as the most suitable coastal protection structure according to the selection criteria and the analyzed conditions. The breakwater is planned to be constructed at an elevation of 5 meters, prior to the wave breaking point. Two breakwaters will be built: the first with a length of 800 meters and the second with a length of 1,000 meters. The design water level (DWL), obtained as approximately 1.26 m, is used to calculate the crest elevation of the breakwater for each armor layer type, namely natural stone, concrete cube, and geobag. The calculated crest elevations are consistent with the Irribaren number, where the wave run-up value depends on the type of armor layer. For the natural stone armor layer, the crest elevation is 3.76 m. For the concrete cube armor layer, the crest elevation is 3.00 m. For the geobag armor layer, the crest elevation is 3.60 m. These variations arise from the different wave propagation and run-up characteristics associated with each material type. Table 8 presents the recapitulated results of the breakwater crest elevation calculations.

Table 8. Recapitulation of Breakwater Elevation

Description	Symbol	Natural Stone	Concrete Cube	Geobag	Unit
Return Period	KT	50	50	50	Year
Design Wave Height	H'0	1.64	1.64	1.64	m
Slope 1:2		0.5	0.5	0.5	
Slope Angle	θ	0.5	0.5	0.5	º
Deep Water Wavelength	L0	52.64	52.64	52.64	m
Irribaren Number	Ir	2.8	2.8	2.8	
Wave Run-Up	Ru/H	1.22	0.76	1.125	
A. Run Up	Ru	2	1.24	1.84	m
Freeboard Height	Fb	0.5	0.5	0.5	m
Design Water Level	DWL	1.26	1.26	1.26	m
Foundation Depth		5.0	5.0	5.0	m
Breakwater Crest Elevation		3.76	3.0	3.60	m
Breakwater Height		8.76	8.0	8.60	m

The dimension calculations for the three types of armor layers, using Equations (19) through (23), are presented in Table 9. Based on these calculations, the breakwater cross-sections are illustrated in Figures 6, 7, and 8.

Table 9. Recapitulation of Breakwater Dimensions

Description	Natural Stone	Concrete Cube	Geobag	Unit
Elevation Puncak	3.76	3.0	3.60	Year
Crest Width	2	1.8	2.80	m
Layer Thickness 1	1.40	1.3	-	m
Layer Thickness 2	0.65	0.6	-	m
Stone Diameter Layer 1	0.6	0.6	-	m
Stone Diameter Layer 2	0.3	0.25	-	m
Stone Diameter Layer 3	0.12	0.1	-	m
Toe Protection Thickness	1	1	-	m
Toe Protection Length	6.5	6.5	-	m
Slope Structure		1:2		
HHWL	0.63	0.63	0.63	m
DWL	1.26	1.26	1.26	m
Depth Kaki Structure	5	5	1.26	m
Wave Height	1.64	1.64	1.64	m
Breakwater Height	8.76	8	8	m

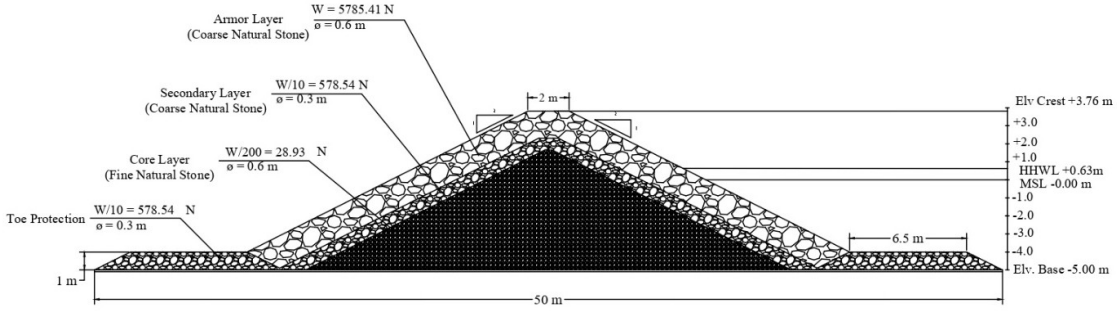

Figure 6. Cross Section of Breakwater with Natural Stone Armor Layer

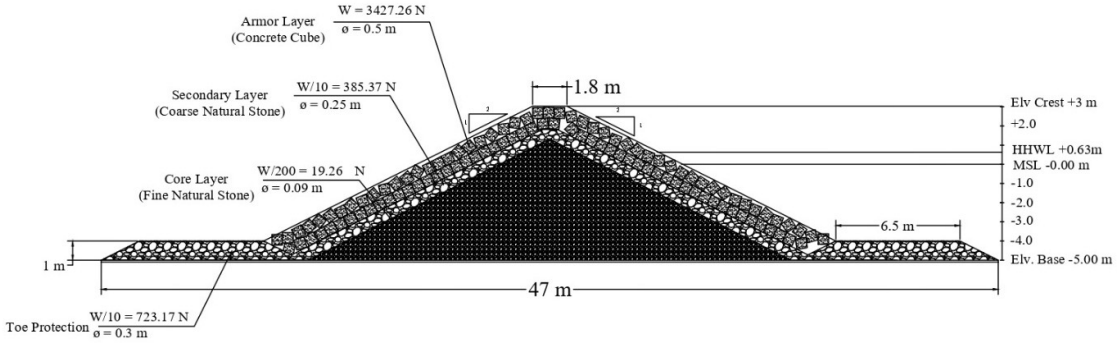

Figure 7. Cross Section of Breakwater with Concrete Cube Armor Layer

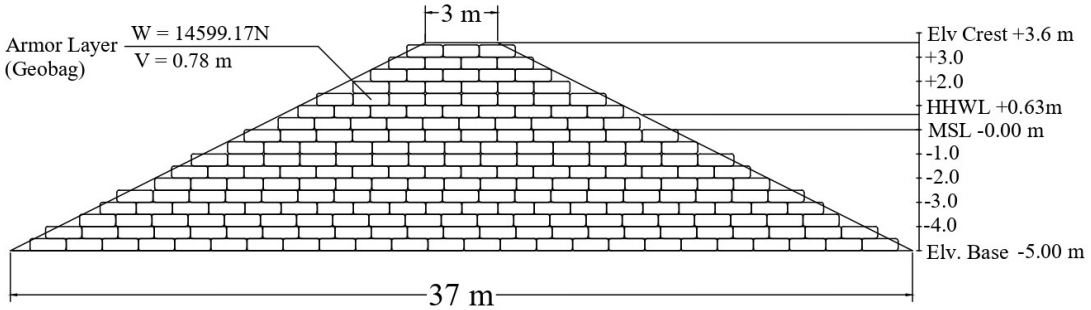

Figure 8. Cross Section of Breakwater with Geobag Armor Layer

Based on the results of the elevation and dimension calculations for the three armor layer types, the breakwater structure shows differences in crest elevation. The natural stone armor layer has a crest elevation of 3.76 m, the concrete cube armor layer reaches 3.00 m, and the geobag armor layer reaches 3.60 m. These differences are due to the unique characteristics of each armor type in dissipating wave energy acting on the breakwater. Each armor layer type also has different dimensions, adjusted according to its specific weight, armor layer coefficient, and the planned transformation wave height. The natural stone armor layer has a crest width of 2.00 m with a first-layer thickness of 1.40 m and a second-layer thickness of 0.65 m. The concrete cube armor layer has a crest width of 1.80 m with a first-layer thickness of 1.30 m and a second-layer thickness of 0.60 m. The geobag armor layer has a crest width of 2.80 m and consists of a single layer only. For all armor layer types, the toe length is 6.50 m and the toe thickness is 1.00 m. The selection of the armor layer type for the breakwater was based on efficiency in dissipating wave energy, cost-effectiveness, and the availability of quarry materials.

Terzaghi stability is highly beneficial in designing coastal protection structures, as it helps ensure that the structure can remain stable on the seabed against currents and pore water pressure. In this study, the geobag armor layer was not considered because it uses only one layer. In Terzaghi stability analysis, a comparison is made between the stone diameters of the armor layer (first layer) and the secondary layer (second layer). Table 10 is the recapitulation of armor stability results.

Table 10. Recapitulation of Armor Stability

Description	Natural Stone	Concrete Cube
Breakwater Filter Rule	2	2.4

Based on the calculations, the ratio between the armor layer diameter and the secondary layer diameter was found to be 2.4, which satisfies the Terzaghi stability requirement that the ratio must be no less than 1.5 and no greater than 3. This result indicates that both armor layer types analyzed are capable of preventing excessive water flow through the structure, thereby ensuring stability and safety.The calculated hydrodynamic parameters provide important insights into the design requirements of the breakwater. The significant wave height (Hs = 1.92 m) and wave period (Ts = 6.99 s) indicate the presence of moderate to high-energy waves, which impose substantial dynamic loading on the structure. The design water level (DWL = 1.26 m) combined with the calculated run-up values defines the critical freeboard requirement; inadequate crest elevation would increase overtopping and accelerate structural degradation. Thus, the crest elevations proposed for each design option are not arbitrary but represent the minimum thresholds necessary to ensure functionality and service life under the local

conditions. The comparative results also demonstrate that differences in armor type lead to distinct performance characteristics. The natural stone design, with crest elevation 3.76 m, provides a greater safety margin against overtopping, although the larger volume and weight of stone may result in higher transport and placement demands. The concrete cube alternative offers a more compact crest elevation (3.00 m) and reduced material volume, which improves constructability, but the higher unit cost must be considered. Geobags, with crest elevation 3.60 m, offer advantages in terms of ease of installation and adaptability, yet their long-term durability and vulnerability to puncture raise maintenance concerns.

From the perspective of stability analysis, the diameter ratios of 2.0 (stone) and 2.4 (concrete cubes) fall well within the acceptable Terzaghi range of 1.5–3, confirming that both designs meet internal stability requirements. This further validates that seepage and internal erosion are not expected to compromise structural integrity.

However, the trade-off between hydraulic performance, construction cost, and material availability suggests that the choice of armor should be tailored to site-specific priorities, whether emphasizing long-term resilience, ease of construction, or economic efficiency. Overall, the discussion demonstrates that the design parameters not only satisfy theoretical stability criteria but also carry practical implications for performance. Cost and sustainability, thereby strengthening the engineering relevance of the results.

4. CONCLUSIONS

The breakwater design is based on a significant wave height of 1.92 m, a wave period of 6.99 s, and a calculated Design Water Level (DWL) of 1.26 m at a site depth of 5 m. Three armor layer types were analyzed: Natural stone: crest elevation 3.76 m, crest width 2.0 m, layer thicknesses 1.50 m and 0.65 m, stone diameters 0.60 m and 0.30 m. Concrete cubes: crest elevation 3.00 m, crest width 1.80 m, layer thicknesses 1.30 m and 0.60 m, equivalent diameters 0.60 m and 0.25 m. Geobags: crest elevation 3.60 m, size 1.50 × 1.00 × 0.50 m, single layer. Terzaghi stability analysis yielded diameter ratios of 2.0 (natural stone) and 2.4 (concrete cubes), both within the acceptable range (1.5–3). These results confirm that all armor types can resist seepage and prevent internal erosion, ensuring the overall safety of the breakwater structure. The verification of calculations was carried out by benchmarking against established coastal engineering standards, where run-up and overtopping were validated with EurOtop (2018) and Goda, armor layer dimensions were checked against the SPM/CERC (1984) as well as the Hudson and Van der Meer equations, and internal stability was assessed using Terzaghi's criteria. At each stage, unit consistency checks and simple uncertainty propagation were applied to evaluate the influence of variations in Hs, Ts, and DWL on crest elevation (Δcrest) and safety margins, thereby ensuring that the design results are technically reliable and robust against data variability.

REFERENCES

[1] D. M. Ashif and A. L. Ahmad, *Prediksi Perubahan Garis Pantai Menggunakan Metode Digital Shoreline Analysis System (DSAS) (Studi Kasus: Wilayah Pesisir Kecamatan Sragi, Lampung Selatan)*, Institut Teknologi Sumatera, 2024.

[2] Universitas Lampung, *Perubahan Garis Pantai di Pesisir Kabupaten Lampung Selatan*, Bandar Lampung, Indonesia: Universitas Lampung, 2022.

[3] N. Rahmawati, M. Khomsin, and N. P. Putri, "Study of coastline changes using remote sensing and GIS in Lampung Province, Indonesia," *Appl. Sci.*, vol. 11, no. 15, p. 6792, 2021.
[4] A. K. Putra, I. Supiyati, and R. A. Pratama, "Analysis of coastal erosion and sedimentation in South Lampung using satellite imagery," *IOP Conf. Ser.: Earth Environ. Sci.*, vol. 1114, no. 1, p. 012018, 2023.
[5] M. Koutsouvela, G. P. Karatzas, and N. C. Zouros, "Functional design of submerged breakwaters for coastal protection using two wave-morphological models," *Coastal Eng.*, vol. 152, p. 103529, Dec. 2019.
[6] H. Saputra and S. Sumiadi, "Prediction of sediment transport due to detached breakwater using Delft3D model," *J. Phys.: Conf. Ser.*, vol. 2763, no. 1, p. 012015, 2024.
[7] M. Vona, M. Cavallaro, and G. Di Paola, "Modeling the effect of breakwaters on coastal morphology using Delft3D-SWAN," *Water*, vol. 12, no. 4, p. 1016, 2020.
[8] J. Shim, K. C. Cho, and Y. H. Kim, "Experimental study on the impact of breakwater geometry on bed morphology and scour," *J. Mar. Sci. Eng.*, vol. 12, no. 12, p. 2174, 2024.
[9] P. Purwanto, R. Tristanto, G. Handoyo, M. Trenggono, and A. A. D. Suryoputro, "Analisis peramalan dan periode ulang gelombang di perairan bagian timur Pulau Lirang, Maluku Barat Daya," *Indones. J. Oceanogr.*, vol. 2, no. 1, pp. 80–89, 2020.
[10] A. R. Dewi and S. Handini, "Analisis data kecepatan angin di Pulau Jawa menggunakan distribusi Weibull," *J. Stat. Apl.*, vol. 6, no. 1, pp. 130–136, 2022.
[11] A. P. M. T. R. Maulidin, "Analisa dimensi dan stabilitas bangunan pengaman (Jetty) Muara Lamteh di Kecamatan Peukan Bada Kabupaten Aceh Besar," B.Eng. Thesis, 2016.
[12] B. Triatmodjo, *Teknik Pantai*. Yogyakarta, Indonesia: Beta Offset, pp. 1–405, 1999.
[13] U.S. Army Coastal Engineering Research Center (CERC), *Shore Protection Manual*, vol. 1. Washington, DC, USA: Dept. Army, 1984.
[14] Y. Goda, *Random Seas and Design of Maritime Structures*. Tokyo, Japan: Univ. of Tokyo Press, 1970.
[15] A. Nugroho and D. H. Ismunarti, "Studi karakteristik dan co-range pasang surut di Teluk," *J. Kelautan*, vol. 4, pp. 93–99, 2015.
[16] F. Dina, O. Nadya, and K. I. Uswatun, "Analisa harmonik pasang surut dengan metode Admiralty pada stasiun berjarak kurang dari 50 km," *J. Meteorol. Klimatol. Geofis.*, vol. 6, no. 1, pp. 38–48, 2019.
[17] T. A. Tarigan, A. L. Ahmad, Suciana, M. A. R. Fauzi, and M. Fatkhurrozi, "Assessment of coastal vulnerability index (CVI) and its application along the Sragi coast, South Lampung, Indonesia," *Int. J. GEOMATE*, vol. 26, no. 116, pp. 134–141, 2024.
[18] "Kajian pengaruh gelombang terhadap kerusakan pantai Matang Danau Kabupaten Sambas," *J. Tek. Sipil*, vol. 11, no. 1, pp. 93–102, 2011.
[19] S. Jonathan, "Perencanaan bangunan pengaman pantai," *J. Univ. Sam Ratulangi*, vol. 21, no. 85, pp. 178–189, 2023.